Wave-vector dependence of intermultiplet transitions in $EuBa_2Cu_3O_x$ ($x=6.1$ and 7): An inelastic neutron-scattering study

U. Staub
Swiss Light Source Project, Paul Scherrer Institute, CH-5232 Villigen PSI, Switzerland

R. Osborn
Material Sciences Division, Argonne National Laboratory, Argonne, Illinois 60439

E. Balcar
Atominstitut der Oesterreichischen Universitäten, A-1020 Vienna, Austria

L. Soderholm
Chemistry Division, Argonne National Laboratory, Argonne, Illinois 60439

V. Trounov
St. Petersburg Nuclear Physics Institute, Gatchina, St. Petersburg, 188350 Russia
(Received 6 September 1996)

The momentum-transfer (Q) dependence of inelastic-neutron-scattering dipolar and higher multipolar CEF split transitions from Eu^{3+} in $EuBa_2Cu_3O_x$ ($x=6.1$ and 7) are calculated and, where possible, compared with the observations. For the transitions between the $^7F_0$ and the $^7F_4$ CEF split multiplets, distinct differences in the Q dependence between the different excitations is anticipated. Some of these transitions are expected to have relatively strong dipolar contributions. In order to perform these calculations, it was necessary to fit the transitions to a model crystal-field splitting scheme in order to determine the eigenfunctions and corresponding energy levels as input for the Q-dependence calculations. We found an unusually low-energy separation between the $^7F_0$ ground state and the first excited $^7F_1$ multiplet which is well understood due to two effects. First, the strong CEF interaction mixes the wave functions of states between different multiplets which leads to a reduction of the energy separation. Second, the free-ion parameters are slightly reduced, which could be understood by assuming a linear behavior with the average distance of the nearest-neighbor shell. [S0163-1829(97)00717-0]

I. INTRODUCTION

It is commonly assumed that the magnetic neutron scattering from noninteracting rare-earth (R) ions has a momentum transfer (Q) dependence that is adequately described by a form factor calculated using the dipole approximation. For scattering arising from within the Russel-Saunders ground multiplet, this is a reasonable assumption, but for spin-orbit transitions between different J multiplets, the Q dependence may be quite different, even for dipole-allowed transitions ($J\rightarrow J\pm1$). If $\Delta J>1$, or ΔL, $\Delta S>0$, the magnetic transitions are nondipolar with zero cross section at $Q=0$ (by definition). A theoretical framework for calculating such cross sections for arbitrary Q ranges has been derived by Balcar and Lovesey[1] and has been compared successfully with the cross section of intermultiplet transitions in a number of f-electron systems.[2,3] However, the theory has not yet been fully tested on transitions between crystal-field-split states in different multiplets. Recently, we have shown that crystal-field transitions can exhibit different Q dependences, even when the transitions involve states within the same multiplet.[4] A full understanding of the Q dependence of crystal-field transitions, both within a single-J multiplet and between different multiplets, would provide a powerful tool for assigning transitions and solving crystalline electric-field (CEF) potentials more reliably. In addition, information otherwise unavailable about free-ion intra-atomic interactions in optically opaque materials, such as metals, would provide insight into their electronic behaviors. Such experiments and calculations will become more common as the flux and resolution of high-energy inelastic neutron spectrometers improve.

In order to investigate the Q dependence of intermultiplet transitions, we have measured the inelastic neutron scattering (INS) of Eu in $RBa_2Cu_3O_x$. Eu was chosen because it has a $J=0$ singlet ground multiplet, with the first excited $J=1$ multiplet at about 44–48 meV, well within the INS accessible energy range. In this relatively low-energy range, it should be possible to resolve transitions to the individual, crystal-field-split states within the $J=1$ multiplet.

We report here the direct determination of intermultiplet transitions in $EuBa_2Cu_3O_x$ ($x=7$ and 6.1) with resolved CEF splittings. The orthorhombic symmetry of the rare-earth site in the $RBa_2Cu_3O_7$ series fully removes the $2J+1$ degeneracy of the multiplets for the non-Kramer ions. The insulating parent compounds ($x<6.4$) have tetragonal R-site symmetry,[5] and therefore some of these singlets merge to doublets. $R=Eu^{3+}$ has a $^7F_0$ ground-state multiplet, which is a nonmagnetic singlet. The first excited $^7F_1$ multiplet is split into three singlets for orthorhombic and a singlet and a dou-

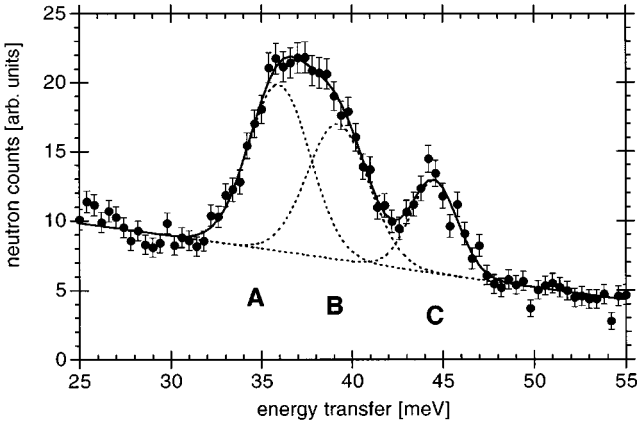

FIG. 1. Energy spectra of neutrons scattered from $EuBa_2Cu_3O_7$ at $T=20$ K, $E_i=80$ meV, and average angle $\varphi=10°$. The solid line corresponds to the fit and the dashed line represents the individual transitions which are labeled $A-C$.

blet for tetragonal symmetry. Because of the low-J value of this multiplet, only the second-order CEF parameters influence the CEF splitting, which permits an accurate determination of these parameters.

Before a full understanding can be attained of the Q dependence to intermultiplet transitions, it is necessary to first have a good estimate of the wave functions and energies of the states involved in the various transitions. There has been considerable work done to determine systematically the CEF splittings of rare-earth (R^{3+}) ions in $RBa_2Cu_3O_7$.[6–10] This work is limited to INS because the materials are opaque to electromagnetic radiation, thereby prohibiting the use of more conventional optical methods. The results have been used to develop models involving charge transfer[8,9] percolative superconductivity[11] coupling of the magnetic response to the CuO_2 states,[12] and R-R exchange interaction.[13] When analyzing the INS data using crystal-field modeling, it has proven necessary to include free-ion parameters in the fitting, particularly for the lighter rare earths where the intermultiplet splittings are relatively small. These free-ion parameters are generally taken directly from the complete work on R:LaF_3.[14]

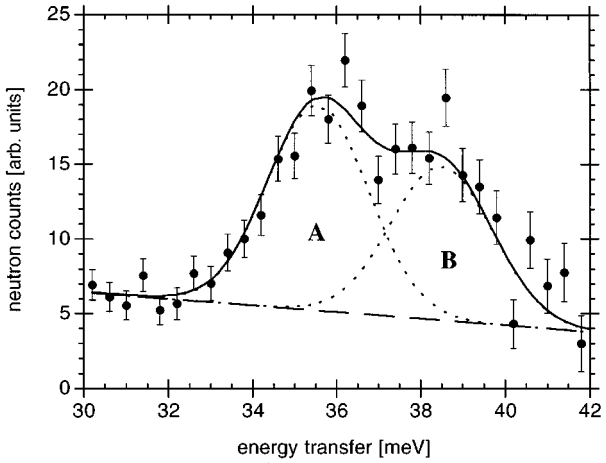

FIG. 2. Energy spectra of neutrons scattered from $EuBa_2Cu_3O_7$ at $T=20$ K, $E_i=50$ meV, and average angle $\varphi=12.5°$. The solid line corresponds to the fit and the dashed line represents the individual transitions which are as in Fig. 1.

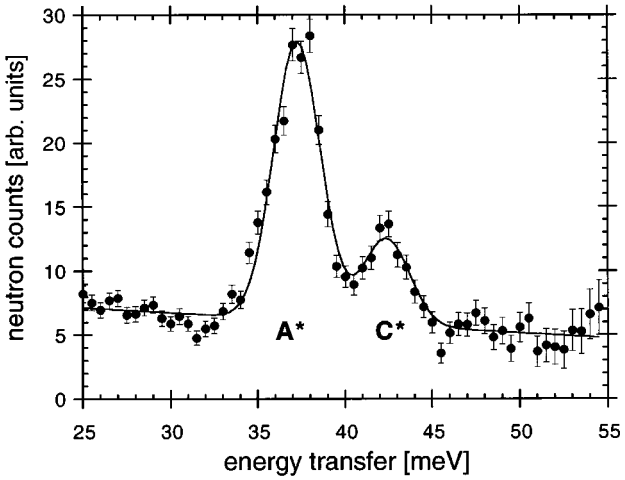

FIG. 3. Energy spectra of neutrons scattered from $EuBa_2Cu_3O_{6.1}$ at $T=20$ K, $E_i=80$ meV, and average angle $\varphi=10°$. The solid line corresponds to the fit. The individual transitions are labeled with A^*,C^*.

The experimental data obtained here from crystal-field-split intermultiplet transitions of Eu provide information about the second-order CEF and the free-ion interaction parameters. We use the results of these fits in theoretical calculations of the Q dependence of the neutron cross section of CEF-split intermultiplet transitions that include both dipolar and higher multipolar transition probabilities. Some preliminary results have been published elsewhere.[4,15]

II. EXPERIMENTS

A 12-g isotope-enriched $^{153}EuBa_2Cu_3O_7$ sample was prepared by standard ceramic techniques. The oxygen content was controlled by heating in the appropriate atmosphere. Neutron diffraction confirmed the single-phase character of the samples. The INS experiments were performed using the low-resolution-medium-energy chopper spectrom-

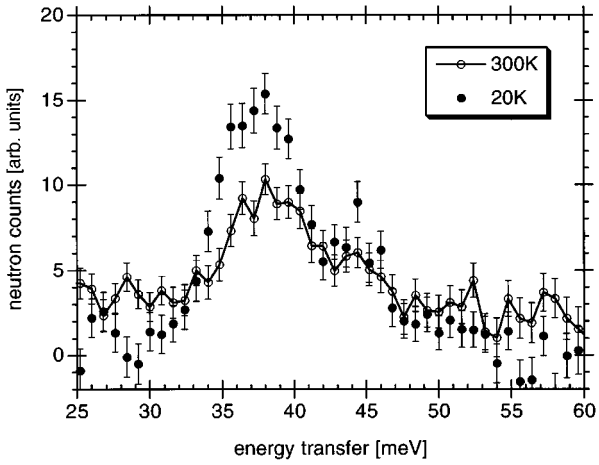

FIG. 4. Temperature dependence of the energy spectra of neutrons scattered from $EuBa_2Cu_3O_{6.1}$. The line is a guide to the eye.

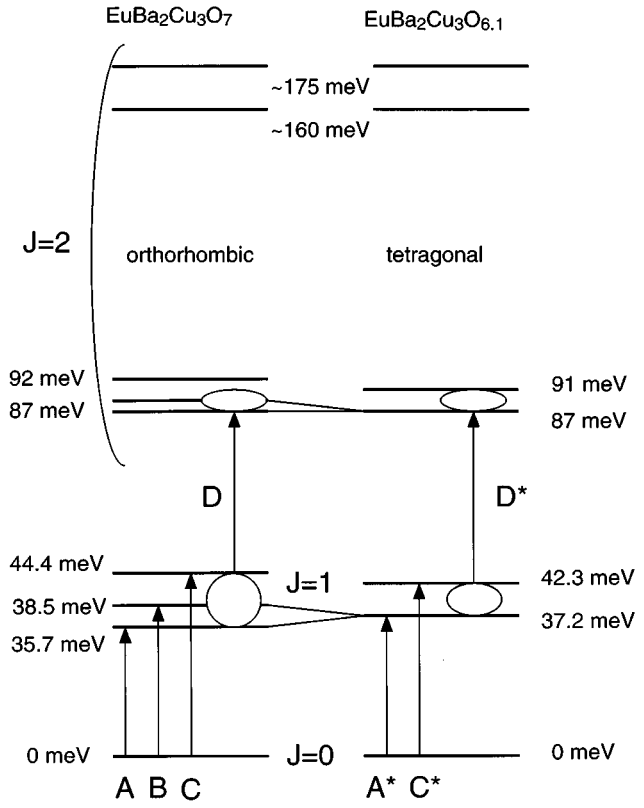

FIG. 5. Energy level scheme of Eu^{3+} in $EuBa_2Cu_3O_x$ ($x=7$ and 6.1) for the three lowest J multiplets. The labels correspond to the transitions shown in the figures, in particular, the label D (D^*) corresponds to several transitions between the first excited $^7F_1$ and the $^7F_2$ CEF-split multiplets.

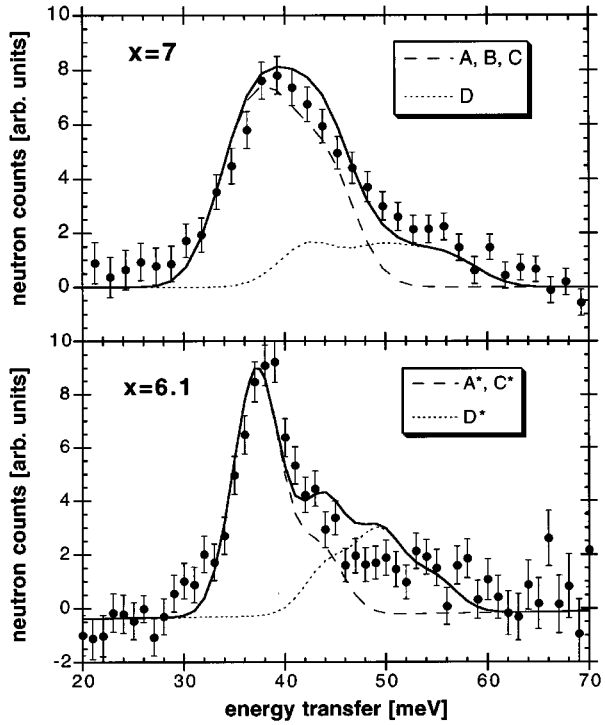

FIG. 6. Background-subtracted magnetic neutron spectra of Eu^{3+} in $EuBa_2Cu_3O_x$. The dashed line corresponds to the $^7F_0$ to $^7F_1$ transitions, the dotted line to the $^7F_1$ to $^7F_2$ transitions, and the solid line to the total calculated intensity derived from the model as explained in the text: upper part, $EuBa_2Cu_3O_{6.1}$; lower part, $EuBa_2Cu_3O_7$.

eter (LRMECS) at the Intense Pulsed Neutron Source (IPNS) at Argonne National Laboratory. The incident neutron energy was chosen to be 50, 60, 80, or 120 meV. The samples were enclosed in flat aluminium containers and then attached to the cold finger of a closed-cycle refrigerator to achieve temperatures of 20 and 300 K. The raw data have been corrected for detector efficiency by standard procedures. The energy-dependent absorption has been measured and was found to be negligible, confirming the high enrichment of the ^{153}Eu isotope. To obtain the magnetic response function of Eu alone, the nonmagnetic contribution to the background was subtracted from the data. This background was estimated using spectra obtained from the same number of moles of $YBa_2Cu_3O_x$, and also the spectrum of an empty sample container.

III. RESULTS

Energy spectra at $T=20$ K are shown in Figs. 1–3 for $EuBa_2Cu_3O_7$, the superconductor, and $EuBa_2Cu_3O_{6.1}$, the insulating parent compound. Three and two well-resolved peaks are observed for the high and low oxygen content compound, respectively. The magnetic origin of these peaks is established by comparing the spectra with those obtained from the non-magnetic Y analogue, as well as by their intensity dependence on temperature, as shown in Fig. 4 for $EuBa_2Cu_3O_7$. These peaks can be assigned to transitions from the $^7F_0$ ground multiplet to the individual CEF split states within the $^7F_1$ first excited multiplet. The energy level scheme for the three lowest J multiplets are shown in Fig. 5. The relatively strong dipolar transitions between $^7F_1$ and $^7F_2$ CEF-split multiplets can be determined by populating the states of the $^7F_1$ multiplet at room temperature (see Fig. 6). However, the individual states cannot be resolved and therefore provide limited information.

The splitting between the $^7F_0$ and the center of gravity of the $^7F_1$ multiplet is 39.5 ± 0.3 meV, distinctly smaller than expected from a comparison with Eu in other oxides, sulphides, and calcogonides, where the splitting is generally in

TABLE I. Averaged energy separation between the $^7F_0$ and $^7F_1$ multiplets for Eu in different host crystals.

Compound	Averaged energy separation between $^7F_0$ and $^7F_1$ (meV)
EuF_3 (Ref. 28)	45.6
Eu $(OH)_3$ (Ref. 28)	46.8
Eu_2O_3 (Ref. 28)	46.2
$EuVO_4$ (Ref. 28)	44.9
$EuPO_4$ (Ref. 28)	46.0
$Eu_2Al_5O_{12}$ (Ref. 28)	43.3
$Eu_2Ga_5O_{12}$ (Ref. 28)	43.2
$Cs_2NaEuCl_6$ (Ref. 28)	44.6
$EuPd_2Si_2$ (metal, $Eu^{+2.7}$) (Ref. 21)	38
$EuBa_2Cu_3O_7$ (this work)	39.5

TABLE II. Averaged energy separation between the $^7F_0$ and $^7F_1$ multiplets for the Eu CEF potential from the RBa$_2$Cu$_3$O$_x$ host. The higher-order CEF parameters from the RBa$_2$Cu$_3$O$_x$ host are $B_0^4=-332$ (meV), $B_2^4=4.5$ (meV), $B_4^4=1.85$ (meV), $B_0^6=53.2$ (meV), $B_2^6=-3.9$ (meV), $B_4^6=213.2$ (meV), and $B_6^6=-0.4$ (meV). The other parameters can be found in the text.

CEF	Spin orbit/Slater integrals	Energy separation (meV)
None	Eu:LaF$_3$/Eu:LaF$_3$	47.4
EuBa$_2$Cu$_3$O$_7$	Eu:LaF$_3$/Eu:LaF$_3$	42.0
None	EuBa$_2$Cu$_3$O$_7$/Eu:LaF$_3$	44.9
EuBa$_2$Cu$_3$O$_7$	EuBa$_2$Cu$_3$O$_7$/Eu:LaF$_3$	39.5
EuBa$_2$Cu$_3$O$_7$	As a function of R	40.2

the range 44–48 meV (Ref. 16) (see Table I). Notably, this splitting is 47 meV for Eu:LaF$_3$, the compound from which the free-ion parameters have been extracted for use in tensor operator calculations. To first order, the experimentally observed energy splittings are determined by the spin-orbit parameter (determining the $^7F_0$ to $^7F_1$ intermultiplet splitting) and two crystal-field parameters, B_0^2 and B_2^2 for orthorhombic symmetry (determining the $^7F_1$ intramultiplet splitting). In addition, the excited transitions between the $^7F_1$ and $^7F_2$ multiplets give further spectroscopic information for a determination of the spin orbit and the fourth-order CEF parameters.

IV. CRYSTAL-FIELD AND FREE-ION INTERACTION

For the analysis of the experimental results a Hamilton operator of the form

$$H=H_{\mathrm{FI}}+H_{\mathrm{CEF}}+H_{\mathrm{cor}} \tag{1}$$

was used. Here, H_{FI} corresponds to the free-ion, H_{CEF} to the crystal field, and H_{cor} to a higher-order correction Hamiltonian. The free-ion Hamiltonian is given as

$$H_{\mathrm{FI}}=\sum_k f_k F^k + A_{\mathrm{SO}}\zeta_f \tag{2}$$

with parameters F^k and ζ_f as Slater-Condon electrostatic and spin-orbit integrals, respectively. f_k and A_{SO} represent matrix elements for the angular parts of these electrostatic and spin-orbit interactions. The CEF Hamiltonian is given as

$$H_{\mathrm{CEF}}=\sum_{q,k,i} B_q^k[C_q^k(i)+C_{-q}^k(i)], \tag{3}$$

TABLE III. CEF parameters derived from EuBa$_2$Cu$_3$O$_7$ and other RBa$_2$Cu$_3$O$_7$ compounds including the $\langle r^{2n}\rangle$ scaled values for Eu.

$x=7$	Eu	Ho (Ref. 9)	Er (Ref. 8)	Nd (Ref. 24)	Gd (Ref. 29)
B_0^2 (meV)	49±1	42±2	33±2	61±3	51
B_2^2 (meV)	5±1	12±1	11±2	3±2	11
$x=6.1$					
B_2^0 (meV)	34±1	17±2	16±1	58±3	

where B_q^k corresponds to the CEF parameters and $C_q^k(i)$ corresponds to spherical tensor operators of rank k, dependent on the ith electron. The correction Hamiltonian, which includes several higher-order terms, is explained in detail elsewhere.[14] The computer code used to determine the different parameters is described by Crosswhite and Crosswhite.[17]

Although, to first order, the splittings of the $^7F_0$ and $^7F_1$ multiplets involve only the second-order CEF parameters and ζ_f, the other free-ion parameters and the higher-order CEF parameters must be included in the fitting in order to obtain reasonable values for the parameters. The higher-order CEF parameters can be approximated by trends across the series[18] and are typified by R=Ho.[9] The extrapolated CEF parameters were obtained by multiplying the parameters from the other rare earths by the ratios $\langle r_{2n}\rangle_{\mathrm{Eu}}/\langle r_{2n}\rangle_R$, where $\langle r_{2n}\rangle$ correspond to the mean radial value of r^{2n} averaged over the atomic wave functions (Table II).[19] It is known that this ratio overestimates the effects of the lanthanide contraction, and therefore an additional antishielding parameter is added for each tensor rank. We decided for simplicity to follow the method previously described by Goodman *et al.*[20] for dealing with this problem.

The small energy separation of the $^7F_0$ and $^7F_1$ multiplets in EuBa$_2$Cu$_3$O$_x$, relative to the separations found in other materials, can be seen from Table I. The small value for EuPd$_2$Si$_2$ is proposed to originate from the intermediate valence character of Eu (Eu$^{2.7+}$).[21] The energy separation between multiplets arises primarily from the free-ion contributions. However, even using the free-ion parameters for Eu:LaF$_3$ (Ref. 14) (see Table II), the average energy separation between the $^7F_0$ and $^7F_1$ multiplets is reduced to 42 meV. This reduced separation is a result of the strong CEF potential of the RBa$_2$Cu$_3$O$_7$ host and originates from the admixture of the wave functions from other J multiplets, as demonstrated in Table II. However, an average separation of 42 meV is not sufficient to fully explain the data. A decrease in the magnitude of the free-ion parameters, compared to the fluoride host, is required for an adequate fit to the data. The fact that the multiplet-energy separation does not depend on the oxygen concentration (compare Figs. 1 and 3) excludes any significant influence due to the metal- (superconductor) insulator transition. In other words, we do not observe a more efficient screening of the Coulomb interaction due to the presence of conduction electrons as has been previously suggested for Pr metal.[3]

As shown in Eq. (2), there are four free-ion parameters that must be considered when modeling the intermultiplet separation, three Slater-Condon electrostatic parameters and one spin-orbit parameter. Because we cannot distinguish between changes arising from electrostatic interactions and those from spin-orbit interactions, we require a model to correlate some of these parameters. The hydrogenic approximation[22] relates the three Slater integrals to each other, reducing to two the number of independent parameters. Recently, it was argued that the spin-orbit parameter and the Slater integrals vary linearly with the average distance of the nearest-neighbor shell,[22]

$$\overline{R}=\sum_i n_i R_i \Big/ \sum_i n_i . \tag{4}$$

TABLE IV. Coefficients of radial integrals times 10^2 in the neutron-scattering cross sections of CEF-split intermultiplet transitions in $EuBa_2Cu_3O_7$. The labels *a*, *b*, *c*, etc., correspond to the same as in Figs. 10 and 11.

E (meV)	$C^{0,0}_{\mu,\nu}$	$C^{0,2}_{\mu,\nu}$	$C^{2,2}_{\mu,\nu}$	$C^{2,4}_{\mu,\nu}$	$C^{4,4}_{\mu,\nu}$	$C^{4,6}_{\mu,\nu}$	$C^{6,6}_{\mu,\nu}$
35.7	78.062	−104.501	35.672	0.459	0.713	0.048	0.272
38.5	74.095	−97.934	32.926	0.387	0.685	0.046	0.256
44.4	68.578	−90.158	30.922	0.807	0.751	0.032	0.344
87	0.055	0.041	1.926	0.169	0.037	0.000	0.104
87	0.005	0.062	2.030	0.212	0.032	0.001	0.132
92	0.000	−0.015	1.935	0.201	0.030	0.000	0.131
168	0.016	0.032	3.192	0.008	0.020	−0.032	0.024
180	0.000	0.000	3.431	0.000	0.030	−0.032	0.028
221 *a*	0.000	0.016	6.675	2.518	0.877	−0.028	0.231
221 *b*	0.001	0.066	6.535	2.596	0.893	−0.019	0.246
234	0.002	0.103	5.129	1.740	0.656	−0.022	0.462
241	0.081	0.060	7.456	5.026	1.131	0.033	0.413
252 *a*	0.082	0.069	7.840	5.452	1.146	0.035	0.310
252 *b*	0.001	−0.009	7.647	5.286	1.117	0.039	0.140
274	0.002	−0.005	8.383	5.242	0.867	0.003	0.045
278	0.000	0.000	0.040	0.022	2.991	0.000	0.343
348	5.414	8.711	5.660	2.005	3.046	0.068	0.168
353 *a*	6.329	9.705	6.002	2.083	2.988	0.046	0.450
353 *b*	6.065	9.884	6.057	1.875	3.010	0.038	0.463
390 *a*	0.000	0.000	0.172	0.131	3.754	0.108	0.175
390 *b*	0.000	0.000	0.661	0.653	3.257	−0.001	0.051
390 *c*	0.019	−0.006	0.465	0.350	3.212	0.040	0.143
390 *d*	0.007	−0.012	0.409	0.282	3.229	0.036	0.140
390 *e*	0.000	0.000	0.002	0.001	3.843	0.138	0.167

Using data obtained from neutron diffraction in this relation, we obtain a value $R=2.4$ Å. This value of R can be used to obtain a spin-orbit parameter of $\zeta_f=162.4$ meV and a free-ion parameter $F^2=10242$ meV. The ratios $F^4/F^2=0.713$ and $F^6/F^2=0.512$ were fixed at the values obtained for $Eu:LaF_3$.[14] The spin-orbit parameter of 162.4 ± 1 meV is comparable to the value of 160.8 ± 1 meV obtained from fitting the energy level scheme and only slightly smaller than the value of 165.9 meV previously determined for $Eu:LaF_3$. The energy splittings derived from the use of Eq. (4) are similar to those derived from fitting the spin-orbit parameter alone, and both models are in reasonable agreement with the observations (see Table III). The best fits from the various models are compared in Table III. We conclude that the reduced average-energy separation between the Eu $^7F_0$ and $^7F_1$ multiplets in $EuBa_2Cu_3O_x$ arises primarily from the mixing of wave functions from the different J multiplets by the strong CEF potential. In addition, a slight reduction of the $Eu:LaF_3$ free-ion parameters is necessary, and arises from the ''small'' average distance of the neighboring oxygen shell.

The second-order parameters obtained for $EuBa_2Cu_3O_x$ are within the range expected based on previously published values for studies of various R (see Table III).[6–10] As a function of oxygen content, the CEF potential exhibits changes reflected by the changes of the observed energy level schemes.[8,9] It is well known that when reducing the oxygen content from $RBa_2Cu_3O_7$ to $RBa_2Cu_3O_6$, there is a transition from the superconducting into the insulation state followed by an orthorhombic to tetragonal structural transition. The second-order CEF parameters decrease by as much as 50% when going from $x=7$ to 6.1, whereas the other parameters do not change by more than 10% (except those which vanish due to symmetry). This change in the magnitude of the second-order parameters as a function of oxygen content, x, is larger for the heavier rare earths, and has almost vanished for $R=$Nd. This is consistent with the observation that the orthorhombic distortion increases with Z.[23] The values of B^2_0 determined here for Eu are consistent with these trends. The results indicate that the differences of the local charge distribution between the low and highly oxygenated samples is larger for the heavier rare-earth ions than for the lighter rare-earth Nd. This result may explain why for $R=$Nd the superconducting transition temperature T_c decreases much more rapidly while reducing the oxygen content, x, sample than for a similar oxygen reduction in the heavier rare-earth samples.[24]

V. HIGHER MULTIPOLAR TRANSITIONS

The calculation of the Q dependence of the CEF-split intermultiplet transitions have been done within the framework introduced by Balcar and Lovesey.[25] The powder-averaged ($|\mathbf{Q}|=Q$) neutron-scattering cross section of a transition between the states μ and ν is proportional to

$$\frac{d\sigma}{d\Omega\, d\omega} \propto \rho_\mu G(Q;\mu,\nu)\,\delta(\hbar\omega + E_\nu - E_\mu). \qquad (5)$$

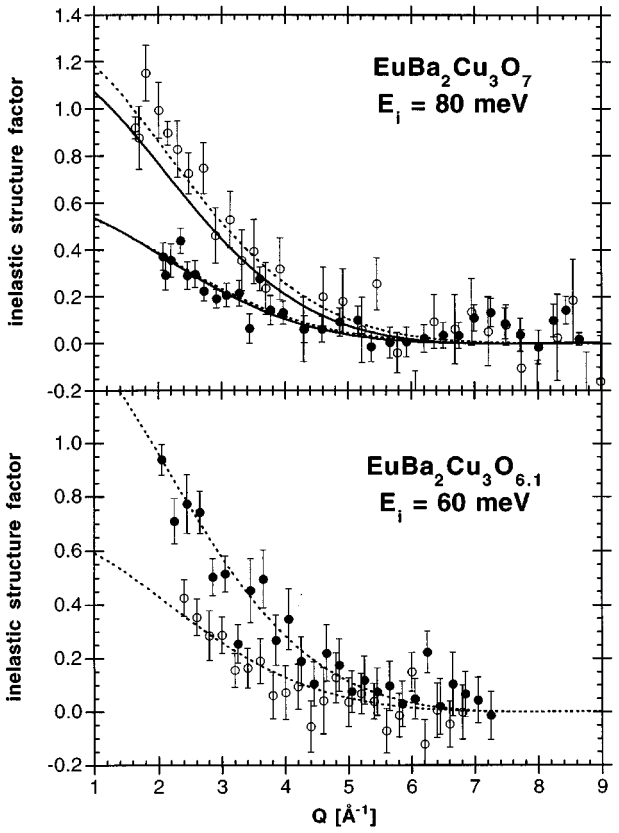

FIG. 7. Q-dependence of the transitions $A+B$ (solid circles) and C (open circles) from the $^7F_0$ ground state into the CEF-split $^7F_1$ multiplet of Eu^{3+} in $EuBa_2Cu_3O_7$ (upper part), and A^* and C^* in $EuBa_2Cu_3O_{6.1}$ (lower part). The dotted line corresponds to calculated individual CEF-split transitions and the solid lines to the pure intermultiplet transitions normalized to the degeneracy of the transition.

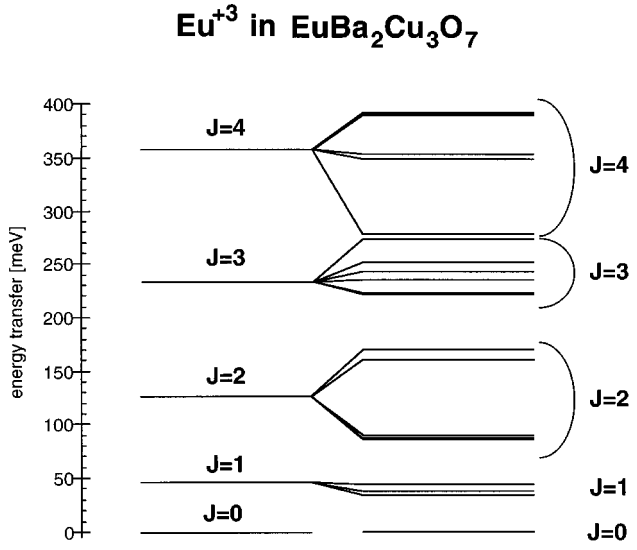

FIG. 8. Energy level scheme of Eu^{3+} in $EuBa_2Cu_3O_7$. The left side corresponds to the free-ion splitting of the J multiplets and the right side to the CEF-split J multiplets.

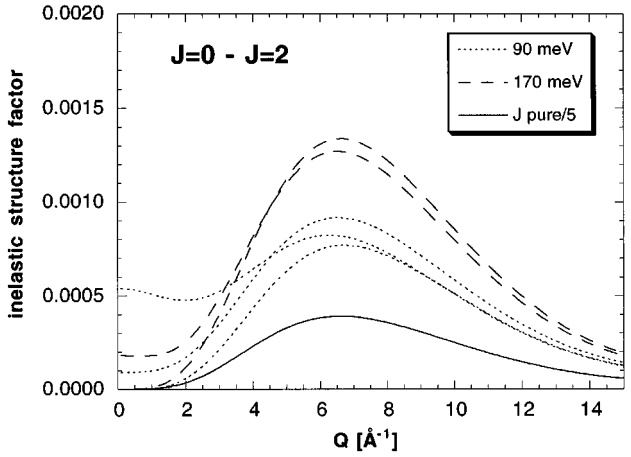

FIG. 9. Calculated Q dependence of the transitions from the $^7F_0$ ground state into $^7F_2$ multiplet of Eu^{3+} in $EuBa_2Cu_3O_7$. The dotted lines correspond to the individual transitions around 90 meV, the dashed lines to the individual transitions around 170 meV, and the solid line to the pure intermultiplet transition per final state.

Here, ρ_μ corresponds to the population factor of the state μ, $\delta(h\omega+E_\nu-E_\mu)$ to the energy conservation law, and $G(Q;\mu,\nu)$ to the inelastic structure factor. The inelastic structure factor can be expressed as

$$\begin{aligned} G(Q;\mu,\nu) = {} & C^{0,0}_{\mu,\nu}\langle J_0(Q)\rangle^2 + C^{0,2}_{\mu,\nu}\langle J_0(Q)\rangle\langle J_2(Q)\rangle \\ & + C^{2,2}_{\mu,\nu}\langle J_2(Q)\rangle^2 + C^{2,4}_{\mu,\nu}\langle J_2(Q)\rangle \\ & \times\langle J_4(Q)\rangle C^{4,4}_{\mu,\nu}\langle J_4(Q)\rangle^2 + C^{4,6}_{\mu,\nu}\langle J_4(Q)\rangle \\ & \times\langle J_6(Q)\rangle + C^{6,6}_{\mu,\nu}\langle J_6(Q)\rangle^2, \end{aligned} \tag{6}$$

where $C^K_{\mu,\nu}$ are constants that depend on the wave functions of the two states. The Q-dependent radial integrals $\langle J_K(Q)\rangle$ are given by

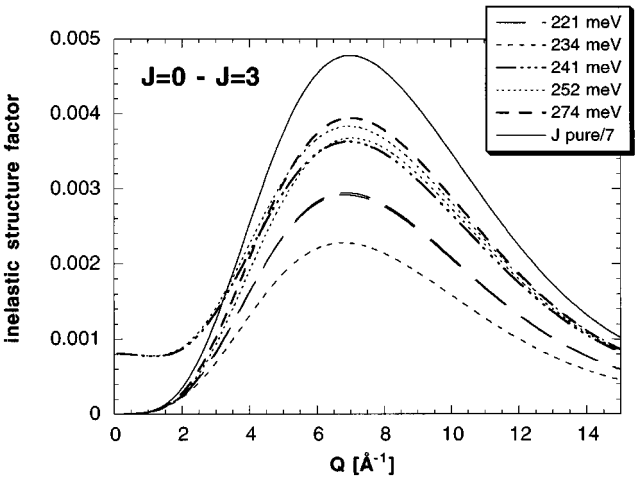

FIG. 10. Calculated Q dependence of the transitions from the $^7F_0$ ground state into $^7F_3$ multiplet of Eu^{3+} in $EuBa_2Cu_3O_7$. The dashed lines correspond to the individual transitions grouped around the energies shown in the legend and the solid line to the pure intermultiplet transition per final state.

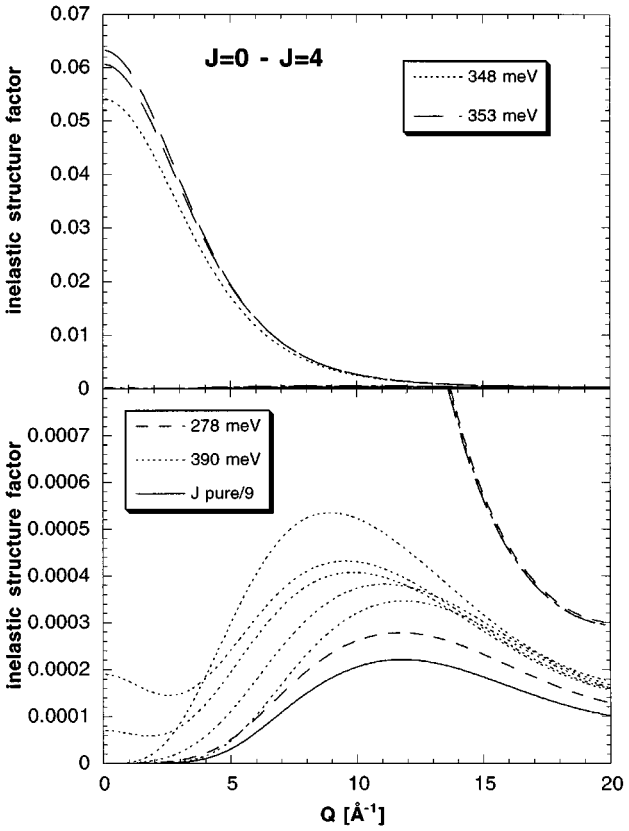

FIG. 11. Calculated Q dependence of the transitions from the $^7F_0$ ground state into $^7F_4$ multiplet of Eu^{3+} in $EuBa_2Cu_3O_7$. The dashed lines correspond to the individual transitions located closely around the energies shown in the legend and the solid line to the pure intermultiplet transition per final state. The lower part is the same figure as the upper part, except an enlargement of the y scale.

$$\langle J_K(Q)\rangle = \int_0^\infty r^2 f^2(r) J_K(Qr)\,dr, \quad K=0,2,4,\ldots, \qquad (7)$$

where $J_K(Qr)$ is a spherical Bessel function of order K and $f(r)$ is the normalized radial part of the one-electron wave function. The $\langle J_K(Q)\rangle$ values have been tabulated for all the rare earths by Freeman and Desclaux[26] using relativistic free-ion wave functions. For this work, we have employed the polynomial approximation introduced by Brown to describe the radial integrals.[27] We note that the structure factor for a transition within the lowest-lying J multiplets is accurately described by the form factor squared. In other words, by assuming that the constants $C^K_{\mu,\nu}$ do not depend on the states μ, and ν and $C^K_{\mu,\nu}=0$ for $k\geq 2$. The inelastic structure factor can then be written as

$$G(Q;\mu,\nu) = f^2(Q) M^2_{\mu,\nu},$$

where $f(Q)$ is the form factor and $M_{\mu,\nu}$ is the transition probability between the two states, e.g., $g_J\langle\mu|J_\perp|\nu\rangle$. In addition to using the CEF potential in the calculations of the inelastic structure factor, which give rise to a state depending $C^K_{\mu,\nu}$ due to the different L,S,J,M quantum numbers for each state, effects of higher-multipolar origin were also included. In other words, the $C^K_{\mu,\nu}$ were extended out to $k=6$.

The first calculations of the inelastic structure factor including the CEF potential were performed on the CEF-split ground-state multiplet in Pr metal because of the simple-cubic symmetry.[3] It was shown that higher multipolar contributions are very small, compared to the total scattering cross section, and could barely be observed by INS. It was also clearly shown that for $Q\neq 0$ there is a nonzero contribution to all the transitions, even those that are dipole forbidden. Different INS studies[2,3] have shown that transitions between different multiplets may have significant higher multipolar contributions.[25]

The calculated inelastic structure factor for the CEF-split $^7F_0$ to $^7F_1$ intermultiplet transitions are compared with the observed spectra for the high- and low-oxygen content samples in Fig. 7. These transitions are strongly dominated by their dipolar contributions. The admixture of the wave functions from higher-lying multiplets results in a slight change of the Q dependence due to small changes of the coefficients $C^K_{\mu,\nu}$, which are tabulated in Table IV. The strongest influence is a small reduction of the overall transition probability $C^0_{\mu,\nu}$.

The energy-level scheme for the five lowest J multiplets, calculated on the basis of our CEF analysis, is shown in Fig. 8. The calculations of the inelastic structure factor for the CEF-split transitions between the $^7F_0$ to $^7F_2$, $^7F_3$, and $^7F_4$ mutliplets are shown in Figs. 9–11. The corresponding $C^K_{\mu,\nu}$ coefficients are also listed in Table IV and the values for the pure intermultiplet transitions in Table V. A comparison of the calculated Q dependences of the transitions for the fully CEF-split model with those determined with the pure quadrupolar intermultiplet model (without CEF), shows an enhancement, by as much as a factor of 2–4, in the cross sections of the CEF-split transitions between $^7F_0$ and $^7F_2$. In addition, some of these transitions exhibit a small dipolar contribution due to the mixing of the wave functions with those from other multiplets. In contrast to the calculations for the $^7F_0$ to $^7F_2$ transitions, the effect on the $^7F_0$ to $^7F_3$ CEF-split transitions is exactly reversed (Fig. 10). In the latter case, the pure intermultiplet transition is distinctly stronger than the CEF-split transitions, which are reduced by 20–60 %. Again, a few transitions exhibit a small dipolar contribution.

The $^7F_0$ to $^7F_4$ transitions exhibit a totally different behavior. As can be seen from Fig. 11, three of the CEF-split transitions have a strong dipolar contribution. This contribution shows a distinctly different Q dependence than the $^7F_0$ to $^7F_1$ transitions. They decrease less with increasing Q, and show a rather conventional form-factor behavior. Such behavior probably originates from an admixture of wave functions from different J multiplets, but with the same quantum

TABLE V. Coefficients of radial integrals times 10^2 in the neutron-scattering cross sections of Eu^{3+} for pure intermultiplet transitions from $J=0$ to J' (1, 2, 3, and 4).

J'	$C^{0,0}_{J,J'}$	$C^{0,2}_{J,J'}$	$C^{2,2}_{J,J'}$	$C^{2,4}_{J,J'}$	$C^{4,4}_{J,J'}$	$C^{4,6}_{J,J'}$	$C^{6,6}_{J,J'}$
1	66.667	−111.111	46.296	0	0	0	0
2	0	0	1.111	0	0	0	0
3	0	0	11.338	6.803	1.020	0	0
4	0	0	0	0	2.525	0	0

numbers L, S, and J in both the initial and the final states. The other transitions are also expected to show some very interesting behavior. Each of these transitions exhibits a different Q dependence due to the distinctly different contributions of the coefficients $C^{K}_{\mu,\nu}$ with the same k (see Table IV). They are all enhanced compared to the pure intermultiplet transition. Therefore, an experimental determination of the Q dependence of these transitions would not only allow an unambiguous assignment to the transitions but also would tremendously increase the experimental information which could remarkably improve the reliability of the determined CEF potential.

VI. CONCLUSIONS

Crystalline-electric-field (CEF) splittings within higher J multiplets have been determined by means of inelastic neutron scattering in $EuBa_2Cu_3O_x$ ($x=6.1$ and 7). The unusually low-energy separation between the $^7F_0$ ground state and the first excited $^7F_1$ multiplet is well understood due to two effects. First, the strong CEF interaction mixes the wave functions of states between different multiplets which leads to a reduction of the energy separation. Second, the free-ion parameters are slightly reduced, which could be understood by assuming a linear behavior with the average distance of the nearest-neighbor shell. The Q dependence of the different dipolar and higher multipolar CEF-split transitions are calculated, and where possible, compared with the observations. For the transitions between the $^7F_0$ and the $^7F_4$ CEF-split multiplets, distinct differences in the Q dependence between the different excitations is anticipated. Some of these transitions are expected to have relatively strong dipolar contributions.

ACKNOWLEDGMENTS

This work was supported by the U.S. DOE, Basic Energy Sciences, and has benefited from the use of the Intense Pulsed Neutron Source at Argonne National Laboratory, all under Contract No. W-31-109-ENG-38.

[1] E. Balcar and S. W. Lovesey, *Theory of Magnetic Neutron and Photon Scattering* (Clarendon, Oxford, 1989).
[2] R. Osborn, S. W. Lovesey, A. D. Taylor, and E. Balcar, in *Handbook on the Physics and Chemistry of Rare Earths*, edited by K. A. Gschneider, Jr. and L. Eyring (North-Holland, Amsterdam, 1991), Vol. 14, p. 1.
[3] A. D. Taylor, R. Osborn, K. A. McEwen, W. G. Stirling, A. A. Bowden, W. G. Williams, E. Balcar, and S. W. Lovesey, Phys. Rev. Lett. **61**, 1309 (1988).
[4] U. Staub, R. Osborn, E. Balcar, L. Soderholm, and V. Trounov, Europhys. Lett. **31**, 175 (1995).
[5] J. D. Jorgensen, M. A. Beno, D. G. Hinks, L. Soderholm, K. J. Volin, R. L. Hittermann, J. D. Grace, I. K. Schuller, C. U. Segre, K. Zhang, and M. S. Kleefisch, Phys. Rev. B **36**, 3608 (1987).
[6] A. Furrer, P. Brüesch, and P. Unternährer, Phys. Rev. B **38**, 4616 (1988).
[7] L. Soderholm, C.-K. Long, G. L. Goodman, and B. D. Dabrowski, Phys. Rev. B **43**, 7923 (1991).
[8] J. Mesot, P. Allenspach, U. Staub, A. Furrer, H. Mutka, R. Osborn, and A. Taylor, Phys. Rev. B **47**, 6027 (1993).
[9] U. Staub, J. Mesot, M. Guillaume, P. Allenspach, A. Furrer, H. Mutka, Z. Bowden, and A. D. Taylor, Phys. Rev. B **50**, 4068 (1994).
[10] A. T. Boothroyd, S. M. Doyle, and R. Osborn, Physica C **217**, 425 (1993).
[11] J. Mesot, P. Allenspach, U. Staub, A. Furrer, and H. Mutka, Phys. Rev. Lett. **70**, 865 (1993).
[12] R. Osborn and E. A. Goremychkin, Physica C **185**, 1179 (1991).
[13] U. Staub, F. Fauth, M. Guillaume, J. Mesot, A. Furrer, P. Dosanjh, and H. Zhou, Europhys. Lett. **21**, 845 (1993).
[14] W. T. Carnall, G. L. Goodman, K. Rajnak, and R. S. Rana, J. Chem. Phys. **90**, 3443 (1989).
[15] U. Staub, L. Soderholm, R. Osborn, M. Guillaume, A. Furrer, and V. Trounov, J. Alloys Compd. **225**, 591 (1995).
[16] C. A. Morrison and R. P. Leavitt, in *Handbook on the Physics and Chemistry of Rare Earths*, edited by K. A. Gschneider and L. Eyring (North-Holland, Amsterdam, 1982), Vol. 5, p. 461.
[17] H. M. Crosswhite and H. Crosswhite, J. Opt. Soc. Am. B **1**, 246 (1984).
[18] U. Staub and L. Soderholm (unpublished).
[19] A. J. Freeman and R. E. Watson, Phys. Rev. **127**, 2058 (1962).
[20] G. L. Goodman, C.-K. Loong, and L. Soderholm, J. Phys. Condens. Matter **3**, 49 (1991).
[21] E. Holland-Moritz, B. Braun, B. Roden, B. Perscheid, E. V. Sampathkumaran, and W. Langel, Phys. Rev. B **35**, 3122 (1987).
[22] Y. R. Shen and W. B. Holzapfel, Phys. Rev. B **52**, 12 618 (1995).
[23] M. Guillaume, P. Allenspach, J. Mesot, B. Roessli, U. Staub, P. Fischer, and A. Furrer, Z. Phys. B **90**, 13 (1993).
[24] P. Allenspach, J. Mesot, U. Staub, M. Guillaume, A. Furrer, S. I. Yoo, M. J. Kramer, R. W. McCallum, H. Maletta, H. Blank, H. Mutka, R. Osborn, M. Arai, Z. Bowden, and A. D. Taylor, Z. Phys. B **95**, 301 (1994).
[25] E. Balcar and S. W. Lovesey, J. Phys. C **19**, 4605 (1986).
[26] A. J. Freeman and J. P. Decleaux, J. Magn. Magn. Mater. **12**, 11 (1979).
[27] P. J. Brown, in *International Tables of Crystallography*, edited by A. J. C. Wilson (Kluwer Academic, Dordrecht, 1992), Vol. C, p. 391.
[28] C. A. Morrison, in *Lecture Notes in Chemistry*, edited by G. Berthier *et al.* (Springer-Verlag, Berlin, 1988), Vol. 47, p. 119.
[29] E. E. Alp, L. Soderholm, G. K. Shenoy, D. G. Hinks, D. W. C. II, K. Zhang, and B. D. Dunlap, Phys. Rev. B **36**, 8910 (1987).